

# Impact of Rain Weather Conditions over Hybrid FSO/58GHz Communication Link in Tropical Region

Ali Jasim Mohammed<sup>\*</sup>, Alaa Hussein Abdulaal<sup>\*\*</sup>, Jafri Din<sup>\*\*\*</sup>, Ahmed Naji Zaidan<sup>\*\*\*\*</sup>, Riyam Ali Yassin<sup>\*\*\*\*\*</sup>, Lam Hong Yin<sup>\*\*\*\*\*</sup>, Suhail Najm Abdullah<sup>\*\*\*\*\*</sup>

<sup>\*</sup> Department of Electrical Engineering, Al-Iraqia University, Iraq  
Eng.AliJasimMohammed@gmail.com  
<https://orcid.org/0009-0008-0756-1157>

<sup>\*\*</sup> Department of Electrical Engineering, Al-Iraqia University, Iraq  
Department of Electrical Engineering, Urmia University  
Engineerlaahussein@gmail.com  
<https://orcid.org/0000-0003-2316-2822>

<sup>\*\*\*</sup> Department of Electrical Engineering, Universiti Teknologi Malaysia (UTM)  
jafri@utm.my  
<https://orcid.org/0000-0001-9129-9826>

<sup>\*\*\*\*</sup> Department of Electrical Engineering, Al-Iraqia University, Iraq  
Ahmednajizaidan@aliraqia.edu.iq  
<https://orcid.org/0009-0007-6361-3786>

<sup>\*\*\*\*\*</sup> Department of Electrical Engineering, Urmia University  
RiyamAliYassin@gmail.com  
<https://orcid.org/0009-0004-1202-0380>

<sup>\*\*\*\*\*</sup> Department of Electronic Engineering Technology, Universiti Tun Hussein Onn Malaysia  
Hylam@uthm.edu.my  
<https://orcid.org/0000-0002-5528-4130>

<sup>\*\*\*\*\*</sup> Department of Electrical Engineering, Al-Iraqia University, Iraq  
suhail.n.abdullah@aliraqia.edu.iq  
<https://orcid.org/0000-0003-4897-9396>

## Abstract

Free Space Optics (FSO) is a potential optical technique poised to complement traditional wireless communication. Using optical signals for point-to-point transmission, FSO offers advantages such as abundant unregulated bandwidth, high data rates, enhanced security, and lower costs than microwave links. However, attenuation due to weather conditions, particularly rain, poses a significant challenge to both FSO and RF transmission. This study proposes a Hybrid FSO/58GHz system model to address rain-induced attenuation, implementing the ITU-R FSO prediction model in Kuala Lumpur to evaluate performance in Malaysia. Utilising three years of rain intensity data from UTM, Kuala Lumpur, the study computes rain attenuation for an FSO link with a 780 nm wavelength based on the ITU-R P.1814 model. Specific attenuations for various RF frequencies are also estimated to identify a suitable frequency for the hybrid system. The study analyses the impacts of channel attenuations on both FSO and RF links to enhance system availability and data rate. Key performance metrics such as received power ( $P_r$ ), signal-to-noise ratio (SNR), and bit error rate (BER) are assessed for a 1 km link. The results demonstrate the successful implementation of the FSO link based on the ITU-R model in Malaysia, identifying 58GHz as the optimal RF frequency for the hybrid system and improving performance under heavy rain conditions.

**Keywords**- FSO, Rain Attenuation, Hybrid FSO/RF, Rain Intensity.

## I. INTRODUCTION

FSO, commonly called optical wireless, is a sort of wireless technology that describes obtaining optical communication by transmitting modulated visible and infrared beams through the atmosphere, which is applied in 5G and 6G technologies. In FSO

frequencies, optical signals are employed as the carrier for point-to-point communication information transmission [1-4]. For wireless communication systems, FSO has offered a superior substitute that is less expensive than radio frequency (RF) links, easier to install, and capable of quickly transferring large amounts of data [5]. Despite all of the benefits fibre optic and microwave systems offer, weather conditions appear to have a greater impact on fibre optic systems than other communication media. A significant party to the existence and consistency of the FSO system is operated by the regional disintegration station [6].

FSO systems are particularly vulnerable to weather fluctuations like rain, fog, and snow, which can significantly affect the signal quality. This limitation must be considered when deploying FSO technology for communication purposes. The rainy season lasts all year round in tropical regions like Malaysia. Rain, therefore, has a major role in signal attenuation and distortion in receiver systems [7]. The most well-known example of a hydrometeor in a mild climate is rain. The primary factor limiting the availability of FSO links is the local weather. In the atmosphere, attenuation can range from a few dB to many dB. FSO is attenuated by both raindrop energy absorption and laser beam scattering in all directions [8-10]. FSO link availability is expected to be limited due to heavy rain. Based on measurements from France and Japan, the ITU-R put up a few prediction models [11]. The rain rate defines the amount of attenuation that any microwave link is expected to experience. For the rain to be felt, the tropical region is identified by intensely heavy rainfall and huge raindrop sizes [12-17]. The ITU-R has developed a scientific approach to predict the amount of RA on any terrestrial radio link [18]. High bits per second and a line of sight are required for radio frequency systems that operate at range (40–43 GHz). There is less radio frequency link availability during periods of severe rain. The application of hybrid FSO/RF, which combines microwave and FSO links, thus has the benefit of improving link availability, which has increased from 99.9547% to 99.9989% [19]. In Graz, Austria, researchers have examined how rain attenuations affect FSO and RF links [20]. Their research is based on the ITU-R P.1814 model [11], which establishes a relationship between certain attenuations and varying rain rates. Rain attenuation is constant, particularly for frequencies greater than 60 GHz. Nonetheless, with rain intensities up to 155 mm/h, the RF link operating below 10 GHz predicts attenuation is less than 10dB/km. When choosing a backup link for the FSO main link in a hybrid system, it is important to consider the least amount of weather attenuation feasible to ensure high availability. This information may be helpful in this regard. The FSO link's rain attenuation in Austria has been estimated based on France in the ITUR model. RA for the FSO link is independent of wavelength, but this is not for the RF link [21]

In [22], the authors investigated the functionality of a hybrid (FSO/RF) model using receiver diversity combining methods. The hybrid model transmits the data and data rate simultaneously via the FSO and RF channels. BER and outage probability are computed using new mathematical techniques. These equations are used to examine how the system performs in the presence of both air turbulence and meteorological variations.

Analysis of an adaptive hybrid FSO/RF model for both the BER and the power received is conducted using the model described in [23], taking into account the effects of fog, humidity, and rain at three wavelengths (850 nm, 950 nm, and 1550nm) for the FSO channels and 10 GHz for the RF link. The findings show that the suggested system performs 49.6%. In addition, the model effectively reduced channel attenuation. It ensured that sufficient power, a high data rate, and a low BER were transmitted to the receiver.

In [24], empirical models are improved to forecast the hybrid FSO/RF and RF for channels with lengths as far as 5 km. The systems are based on long-term data on air attenuations from the tropical climatic zone. For frequency bands up to 100 GHz, the ITU-R rain attenuation model is used to build the RF link availability forecast model.

According to [25], signal wavelengths and link distances are the main system components contributing to this. It has been discovered that modifying the operational wavelength and connection distance could enhance the transmission of the hybrid FSO/RF system's link quality. Link budget analysis, which compares the implications of the theoretical and practical systems, is provided in various tabular forms.

The performance of a hybrid FSO/RF model is looked at in [26] in relation to weather-related losses and air turbulence. While the FSO link uses a multi-pulse position modulation approach to follow the Malaga distribution, the RF link uses 16 quadrature amplitude modulation to follow the Rice distribution. New formulae for BER and outage probability are produced for RF, FSO, and hybrid FSO/RF systems. The outage probability of the FSO connection alone drops to around  $10^{-5}$  with implementing the hybrid FSO/RF link from about  $10^{-2}$ . The authors of [27] provide a simulated study under climatic circumstances in the capital province of Punjab, Lahore. Calculations are made for the link's SNR, BER, and Pr. Improving Pr, which is closely related to transmitted power, may improve the performance assessment variables (SNR, BER, LM, and Data Rate).

Air attenuation is simulated against the performance assessment variables. Using these data statistics, they can develop an adaptive and switching approach to improve an FSO link's availability and performance. According to the Pr for 1 Gb/s data rate, SNR and BER are calculated for connection lengths (0.2 km, 0.5 km, and 1 km) for 4 Pulse Amplitude Modulation (PAM). This modelling of a hybrid communication system is done in [28]. With a BER of  $10^{-10}$  at a 0.5 km connection length, mmWave/THz carrier is shown to be suitable for changeable fog conditions. With a BER of  $10^{-8}$ , FSO performs well for varying rain rates. In both communication systems, increasing transmit power may improve the link length and performance. The THz carrier provides high data rates, and an FSO/THz model is suggested to provide dependable communication under adverse weather conditions. The authors in [29] thoroughly analyse a hybrid (FSO/RF) system with 320 Gbps channel capacity. In order to enhance the performance of the system, the receiver system employs a digital signal processing (DSP) correction mechanism alongside 256-quadrature amplitude modulation (QAM) that is separated into channels using circular polarisation division multiplexing (CPDM). The effect of weather on link attenuations is documented in [30], based on real data in which the physical pathways were near-coincident and the RF was in the E band. All these related works are presented in TABLE I, which includes a state-of-the-art summary.

TABLE 1. SUMMARY OF RELATED WORKS FOR PERFORMANCE EVALUATIONS OF FSO/RF HYBRID SYSTEMS.

Ref.	Year	Aim	Contribution of the Research
[20]	2009	Performance Evaluation under fog, rain, and snow weather conditions.	Prediction of specific attenuations of fog, rain, and snow.
[22]	2019	Performance Analysis under rain and fog weather conditions.	Average BER and outage probability estimation.
[23]	2020	Examination of the FSO's performance at various wavelengths in the presence of rain, humidity, and fog.	Received power and the BER are obtained.
[24]	2020	System availability under tropical rain conditions.	Investigation of outage probability and link availability in tropical Malaysia.
[31]	2020	Performance Analysis under Atmospheric Turbulence	Evaluation of outage probability and BER for the proposed model.
[25]	2020	Link budget analysis under rain and fog factors.	The $P_r$ of the Hybrid FSO/RF model is investigated.
[27]	2021	Performance Analysis under dust and fog conditions.	SNR, BER, link margin (LM), and data rate are evaluated, proposing algorithm switching between FSO & RF links.
[26]	2022	Performance Evaluation under atmospheric turbulence	Estimation of outage probability and BER
[28]	2023	hybrid FSO/mmWave/THz system under rain and fog conditions.	Received power, SNR, and BER are obtained for a link distance of 0.1, 0.2, and 1 km.
[32]	2023	Performance Analysis dust effects and Gamma-Gamma (G-G) atmospheric turbulence	Estimation of BER, outage probability, and SNR
[30]	2024	Performance Analysis under weather conditions	Investigation of the correlation between the RF and FSO channels by using empirical data.
	Current Paper	Implementation & Evaluation of the performance of FSO/58GHz under tropical rainy channel.	<ol style="list-style-type: none"> <li>1- Prediction of rain attenuation in CCDF based on real data measurements of rain rates.</li> <li>2- Investigation of received power, SNR &amp; BER for RF &amp; FSO to evaluate the performance of Hybrid.</li> <li>3- Proposing algorithm switching dependent on the received power.</li> </ol>

## II. SPECIFIC ATTENUATION OF THE RAIN (Rsa)

In addition to tiny airborne particles like haze and fog, rain is another important transmission impact, particularly in tropical climates. Rain significantly attenuates the operating frequency as it approaches 10 GHz since the operating frequency's wavelength is similar to the size of raindrops. Numerous investigations have been conducted to comprehend the microphysical properties of precipitation and its relationship to electromagnetic wave propagation [33]. The rain forecast is fading. The specific attenuation of the rain determines the characteristics of the terrestrial link, which is derived from ITU-R P. 838-3 [34] or modified by the spread of DSD data. Rain attenuation depends on the polarisation types, transmission frequency, and the magnitude and shape of the rainfall. The rain-specific attenuation  $\gamma$  is predicted, as in (1) [12-17]:

$$\gamma = 4.343 \times 10^3 \int_0^\infty Q(D)N(D) dD \quad (1)$$

Where  $\gamma$  is the Rsa (dB/km),  $Q$  is the total extinction cross-section area (m<sup>2</sup>), and  $N(D)$  is the drop size distribution (DSD) of the rain (m<sup>-3</sup>mm<sup>-1</sup>).

Indeed, a power law link between rain intensity and Rsa has been identified. The relationship above is primarily derived from the computation of the scattering function and the understanding of the raindrop size distribution (DSD) while accounting for the scattering cross-section of individual particles and the terminal velocity ( $v$  [m/s]). However, it is important to remember that the DSD features could change throughout time, space, and various climate zones. As a result, tropical DSD differs from temperate DSD in terms of microphysical properties [12-17, 35, 36]. Raindrops with a diameter of  $D$  (mm) typically range from 0.1 mm to around 7 mm; drops bigger than these are hydrodynamically unstable and have a tendency to fragment into smaller drops. Such small raindrops are expected to have a major impact on the optical wavelength as their sizes are comparable to the transmitted optical wavelength. The rain-specific attenuation could be determined, as in (2) [11]:

$$\gamma = k.R^\alpha \quad (2)$$

Where  $k$  and  $\alpha$  are the rain coefficients, and  $R$  is the rain rate (mm/h). The features of the rain and some luminosity bending from observations determine the power law values " $k$ " and " $\alpha$ ". The power laws  $k$  and  $\alpha$  regarding customs for estimating the rain attenuations for France and Japan are displayed in TABLE II.

TABLE 2. RAIN COEFFICIENTS FOR FSO IN FRANCE AND JAPAN [11].

Location	The power law 'k' and 'α'	
	k	α
Japan	1.58	0.63
France	1.076	0.67

Free data for particular RA estimations of  $k$  and  $\alpha$  worth for FSO are based on data from temperate countries. The soft station's predicted rain attenuation criterion is unable to effectively predict the inter-tropical vicinity because tropical regions experience higher rates of precipitation than temperate regions. Interferences at the transmission medium can manifest in an unforeseen manner. Weather conditions, including haze, fog, and rain, can cause interference, which can result in the absorption and scattering of transmitted light. Sunlight or scintillation can also have an impact on light transmission. Thus, it's important to take into account any building structures underneath the link that might increase thermal activity in the air and generate scintillation on the signal that is received [37-42].

### III. HYBRID FSO/RF SYSTEM

The suggested approach is used to provide constant high availability. When the FSO link is lost due to high atmospheric attenuation, The RF connection serves as a fallback, as shown in Figure 1. The FSO, RF, and switch are the three sub-systems that make up the system. The suggested approach directly switches to the RF if the  $P_r$  falls below the threshold amount. Once the received optical signal meets the threshold value, the data are then sent across the RF. As a result, the system returns to the FSO connection [23]. This work develops a hybrid FSO/RF model affected by rain-induced attenuation. Based on the ITUR FSO prediction model, the FSO link operates at 780 nm and uses a non-return to zero on-off keying (NRZOOK) modulation technique for the RF connection at 58 GHz. To improve the system's availability and data rate constantly, the impact of channel attenuation on the RF and FSO connections is examined and evaluated. The received power, BER, and SNR are gathered for a one-kilometre connection length to evaluate the suggested system performance.

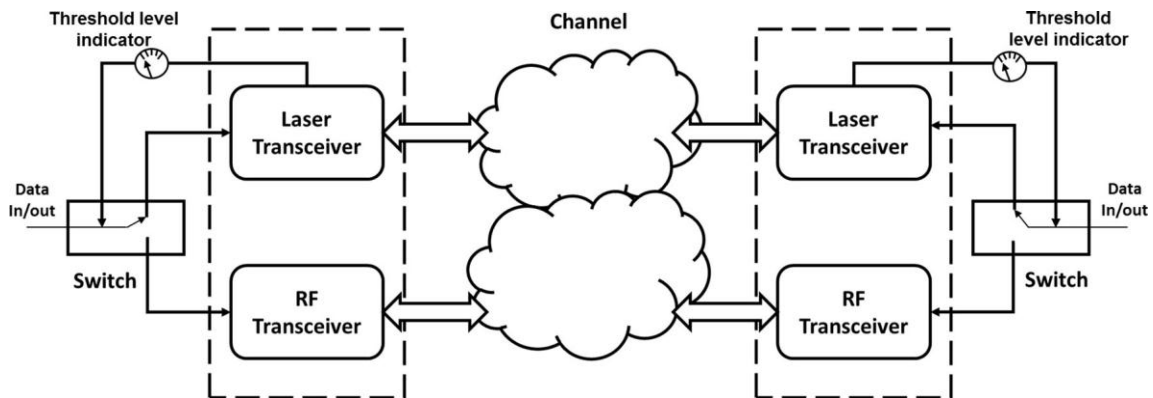


Figure 1. Hybrid FSO/RF System [23].

### IV. PERFORMANCE EVALUATION OF HYBRID FSO/RF

#### A. The Received Power

For an FSO system,  $P_r$  is given in (3) [43]:

$$P_r = P_t \frac{D^2}{\theta^2 L^2} 10^{-\gamma L/10} \tau_{trans} \tau_{rec} \quad (3)$$

Where  $P_t$  is the transmitter power,  $L$  is the path length,  $D$  is the diameter of the receiver,  $\theta$  is the whole divergence angle,  $\gamma$  is the total attenuation factor,  $\tau_{trans}$  and  $\tau_{rec}$  are the transmitter and receiver optical efficiencies, respectively.

In an RF system, the  $P_r$  (4) assumes the transmitter and the receiver have uniform antennas [44].

$$P_r = P_t G_t G_r \tau_{RF} \left(\frac{\lambda}{4\pi}\right)^2 \left(\frac{1}{L^2}\right) \tau_{trans} \tau_{rec} \quad (4)$$

Where  $G_t G_r$  are the gain,  $\lambda$  is the wavelength of the signal,  $\tau_{RF}$  is the RF link attenuation, and  $\alpha$  is the atmospheric attenuation, which are given in (5):

$$\tau_{RF} = 10^{-\alpha L/10} \quad (5)$$

$G_{T/R}$  is the gain of the transmitter and receiver as shown in (6) [44]:

$$G_{T/R} = \left(\frac{\pi D_{T/R}}{\lambda}\right)^2 \quad (6)$$

Where  $D_T$  and  $D_R$  are the optical aperture diameters.

### B. SNR and BER.

IN the FSO system, SNR is given in (7) when using PIN photodiode [45]:

$$SNR_{PIN} = \frac{I_p^2}{2qB(I_p + I_D) + 4KT_{PIN}BF_n/R_L} \quad (7)$$

Where  $I_p$  is the average photocurrent (8),  $q$  is the electron charge,  $B$  is the bandwidth,  $I_D$  is the dark current,  $T_{PIN}$  is the temperature photodiode absolute (K),  $F_n$  is the photodiode noise figure which is equal to 1 for PIN photodiode and  $R_L$  is the PIN load resistor.

$$I_p = P_r R_{PIN} \quad (8)$$

Where  $R_{PIN}$  is the photodetector responsivity.

The BER estimation depends on the modulation method. The OOK modulation method is typically utilised in FSO systems (9) [46].

$$BER_{NRZ-OOK} = \frac{1}{2} \operatorname{erfc} \left( \frac{\sqrt{SNR_{PIN}}}{2\sqrt{2}} \right) \quad (9)$$

For the RF system, the SNR is given in (10) [44, 46]:

$$SNR_{RF} = \frac{P_r/R_{eq}}{4KTBF_n/R_{eq}} \quad (10)$$

Where  $R_{eq}$  is the resistance equivalent,  $K$  is Boltzmann's constant,  $B$  is the bandwidth,  $T$  is the temperature and  $F_n$  is the noise figure for RF receiver. The BER is given in (11) [46]:

$$BER_{RF} = \frac{1}{2} \operatorname{erfc} \left( \frac{\sqrt{SNR_{RF}}}{2\sqrt{2}} \right) \quad (11)$$

### C. Data Collection & Processing

A prior study provided information on measures of rain intensity (mm/h) over three years [47]. The study was conducted at UTM, Kuala Lumpur. The location was selected since it falls inside the study's urban area. DSD measurements were collected between January 1992 and December 1994 using a Joss–Waldvogel disdrometer (JWD, RD-69) that was installed in UTM at an elevation of 35 m above the surrounding sea. By considering an unembellished duration of at least one hour between one enterprise and the subsequent one, 781 fall occurrences were selected from the over 100,512 minutes of rain (one-minute integration repetition) that the disdrometer gave. Throughout the three years, the disdrometer was always functional for at least 98% of the day. The disdrometer is

separated into 20 bins ranging in size from 0.3 to 5.3 mm, with a cross-section area of  $S = 5000 \text{ mm}^2$ . The JW disdrometer's rain intensity reading can be calculated as (12) [38, 48]:

$$R = \frac{3600\pi}{65T} \sum_{i=1}^{20} (D_i^3 n_i) \quad (12)$$

Where  $n_i$  is the falls number,  $T$  is the integration time (sec), and the drop size distribution (DSD) of the rain  $N(D_i)$  is measured as (13):

$$N(D_i) = \frac{n_i \times 10^6}{V(D_i) \times S \times T \times \Delta D_i} \quad (13)$$

Where  $\Delta D_i$  is the width of each drop size bin (mm),  $V(D_i)$  is the terminal velocity (m/s)

$k$  and  $\alpha$  are determined using rain rate data and rain attenuation calculations, which are displayed in TABLE III. In Kuala Lumpur, it displays a few frequencies with both vertical and horizontal polarisations [49].  $k$  and  $\alpha$  for RF lines are also provided by ITUR P.838-3 [34]. The study will focus on estimating a 58 GHz radio link in Kuala Lumpur, Malaysia. Rain Intensity Information gathered from previous studies in FKE and UTM will be used [47]. Thus, the local atmospheric condition (especially rain precipitation) will be seriously considered.

On the other hand, similar work will be conducted on the establishment of FSO links. However, only the ITUR FSO prediction model [11] will be used. Also, a Hybrid FSO/RF will be implemented in Figure 2. First, the threshold value for the switching between a radio link and an FSO link is required to be determined. Time series rain intensity data has been used to promote the hybrid FSO/RF link.

TABLE 3. RAIN COEFFICIENTS FOR FSO FOR VERTICAL AND HORIZONTAL POLARISATIONS IN KL [49].

Frequency (GHz)	Horizontal Polarisation		Vertical Polarisation	
	$K$	$\alpha$	$k$	$\alpha$
10	0.01231	1.219646	0.010478	1.216843
20	0.097033	1.046516	0.089639	1.015352
30	0.227233	0.994813	0.200858	0.977096
40	0.415474	0.92642	0.36615	0.916555
50	0.61878	0.865942	0.550463	0.862389
58	0.752824	0.833201	0.679394	0.831381

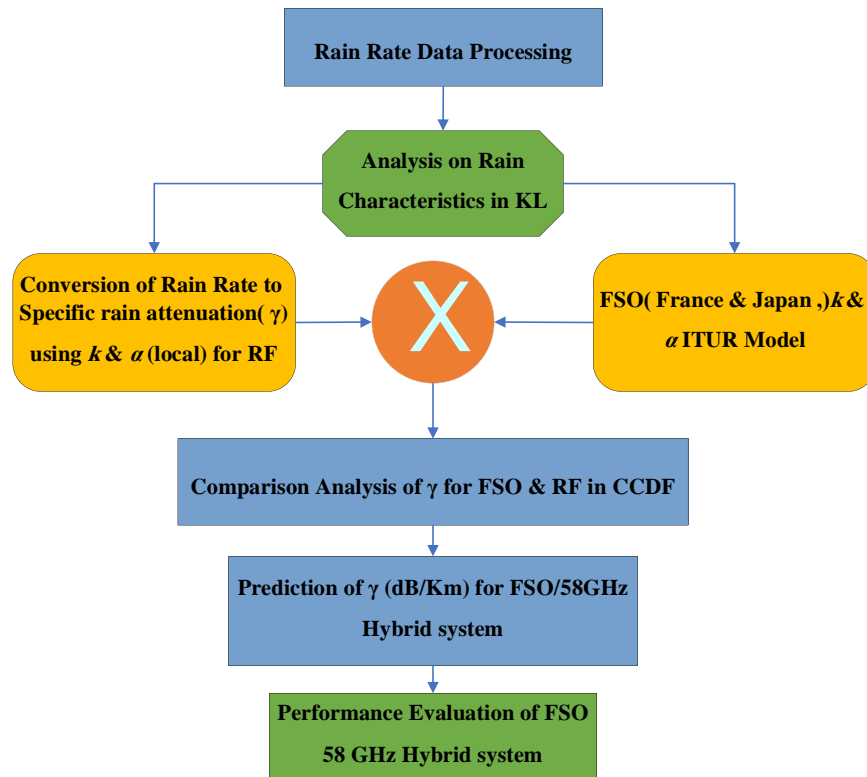


Figure 2. Flow Chart of the Methodology

#### D. Simulation of Proposed Model

The effects of rain on FSO and RF lines while utilising the NRZOOK modulation scheme in the transmitter and a PIN photodiode in the FSO receiver are simulated using MATLAB software. A 1 km connection length is used to simulate the system with transmitter strengths of 5, 10, 50, and 100 mw. The system's received optical power, SNR, and BER are used to assess the effectiveness of the FSO connection. In order to demonstrate the potential for utilising the RF connection as a backup to the FSO link and demonstrate the combined attenuation of rain [50-51], a comparison analysis between the FSO and RF links in the suggested hybrid model is conducted. This study uses Rain Rate measurements throughout three years of data [47]. TABLE IV illustrates all the parameter values for the suggested systems.

TABLE 4. PARAMETERS FOR THE FSO/RF HYBRID SYSTEM [22,23,46].

Parameters for FSO Link		Parameters for RF Link	
Parameter	Value	Parameter	Value
$P_t$	5, 10, 50 and 100 mW	$P_t$	5, 10, 50 and 100 mW
$\theta$	1 mrad	$\tau_{trans}$	0.5
$\tau_{trans}$	0.9	$\tau_{rec}$	0.5
$\tau_{rec}$	0.9	$\lambda$	5.16 mm (58 GHz)
$\lambda$	780 nm	$G_T$	44 dBi
$L$	1 Km	$G_R$	44 dBi
$N_b$	-30 dBm	$S_r$	-110 dBm
$R_L$	1 K $\Omega$	$R_{eq}$	50 K $\Omega$
$k$	$1.38 \times 10^{-23}$ J K	$T$	290 K
$D$	15 cm	$F_n$	5dB
$T_{PIN}$	298 K		
$I_D$	10 nA		

$R_{PIN}$	0.6 A/W	
$B$	0.5 GHz	

### V. RESULTS & ANALYSIS

The Complementary Cumulative Distribution Functions (CCDFs) of rain rate for KL, Japan, and France are shown in Figure 3. The rain intensity of Japan is comparable to the rain rate of KL, or it is almost the same at 0.01% of the time. Therefore, the  $R_{sa}$  for the FSO link has been estimated in Kuala Lumpur based on the data of power law  $k$  and  $\alpha$  for Japan.

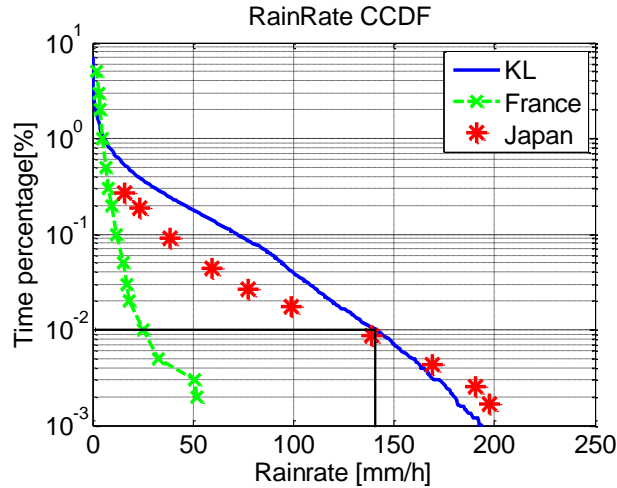


Figure 3. Rain Rate for Kuala Lumpur, France, and Japan.

The average rain rate ( $R_{0.01}$ ) for Japan and Kuala Lumpur is roughly equal to 140 (mm/h) at 0.01% of the time (highest link availability), whereas it is approximately 25 mm/h for France. Figure 4 shows the time series for Kuala Lumpur's rain intensity in minutes. It shows that different times can provide different rain rates. This is because the rain rate data varies from drop size distribution measurements every minute.

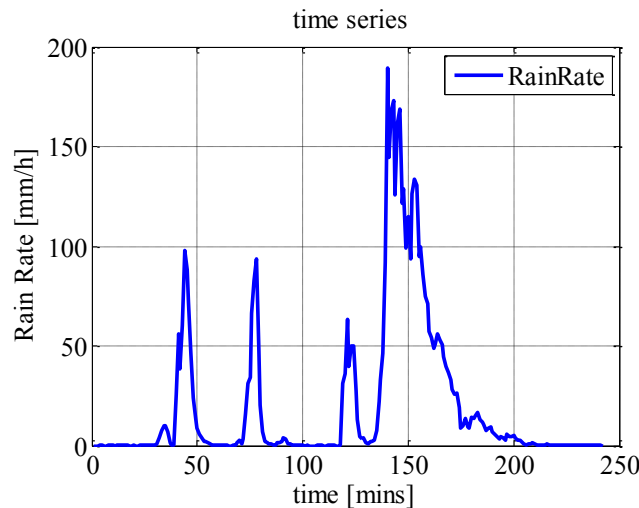


Figure 4. Time Series for Rain Rate in KL

Rain attenuation calculations are done in this study using "(2)", as discussed in section II. Specific rain attenuations have been computed for RF links at 40 GHz and 58 GHz with both polarisations (vertical and horizontal) for ITUR P.838-3 [34] and local data of KL in CCDFs, as shown in Figure 5. ITUR provides lower  $R_{sa}$  values than KL at vertical and horizontal polarisations. This is very predictable given the many DSDs that characterise tropical regions, including medium and big drop sizes with high rain rates. On

another note, the rain attenuation for vertical polarisation is lower than horizontal polarisation for all frequencies. Therefore, it has been estimated that RF links in this study depend on vertical polarisation.

Figure 6 shows the specific rain attenuations in dB/Km for RF links with vertical polarisations at 10, 20, 30, 40, 50, and 58 GHz are approximately equal to 5 dB, 14 dB, 25 dB, 34 dB, 40 dB, and 42 dB respectively. As we can see, the rain attenuation increases with both the intensity and frequency of the rain. It can be insignificant at a frequency of 10 GHz and below. Meanwhile, Figure 7 provides the rain attenuations for FSO links based on the power law  $k$  and  $\alpha$  data in Japan and some RF links (40-58 GHz) with rain rates up to 250 mm/h. As can be seen here, the FSO link provides lower rain attenuation as compared to RF links in high rain rates (up to 250 mm/h). This is because the wavelength of FSO is very small (780 nm) in comparison with raindrops' diameters (100 to 10,000  $\mu\text{m}$ ).

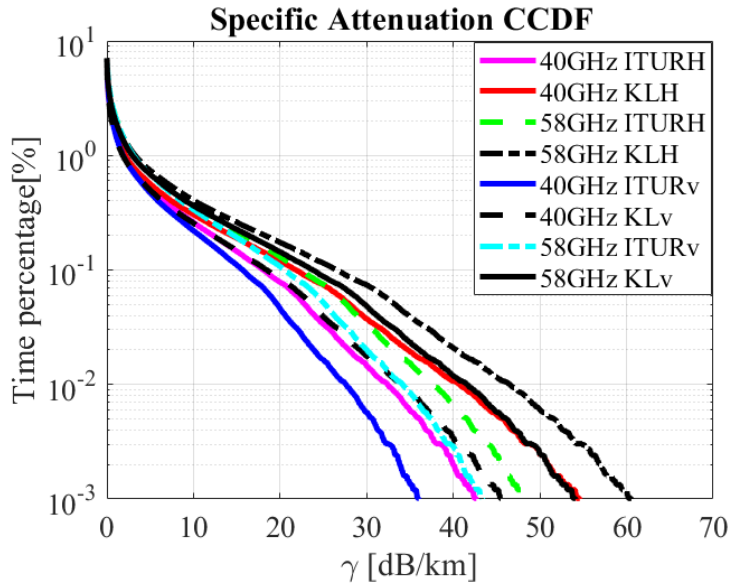


Figure 5. Specific attenuations CCDFs for Vertical and Horizontal polarisations based on ITUR P.383-3 and KL

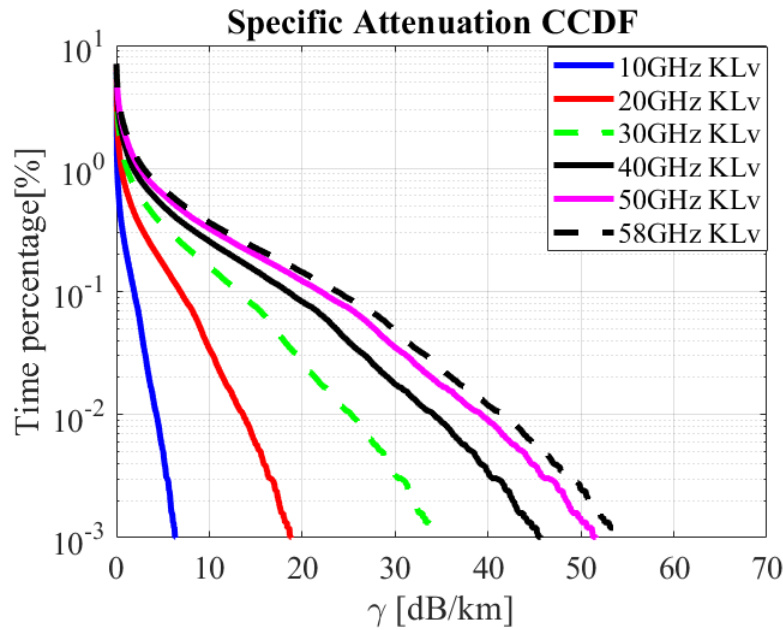


Figure 6. Specific Attenuations CCDFs for RF (10-60) GHz in KL

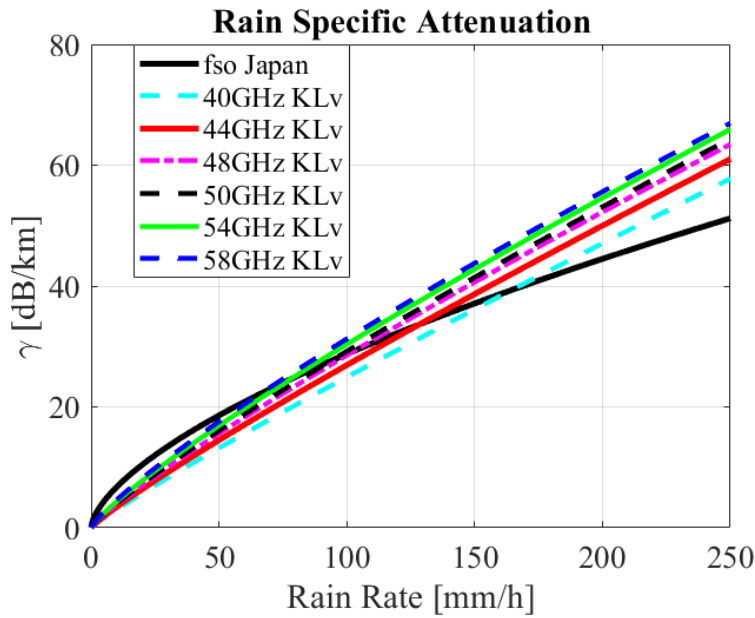


Figure 7. Rain Attenuations for FSO and Some RF Links in KL

Figure 8 compares rain attenuations between 40 GHz and 58 GHz RF links with FSO links. As can be seen, when the rain rate is more than 150 mm/h ( $R > 150$  mm/h), this issue may happen a few times per year. Therefore, selecting 40 GHz as the radio frequency in a Hybrid system is insignificant. On the other hand, when the rain rate is approximately equal to 55 mm/h ( $R = 55$  mm/h), the 58 GHz link can be supplemented with an FSO link as Hybrid FSO/58GHz to increase data rate transmission and improve the performance of the signal under heavy rain condition. The time series in minutes of particular rain attenuations for FSO and RF links at 40 GHz and 58 GHz in KL is shown in Figure 9; the rain rate and the form of the time series of a given RA are similar. This is because rain attenuation depends on rain intensity in relation to frequency.

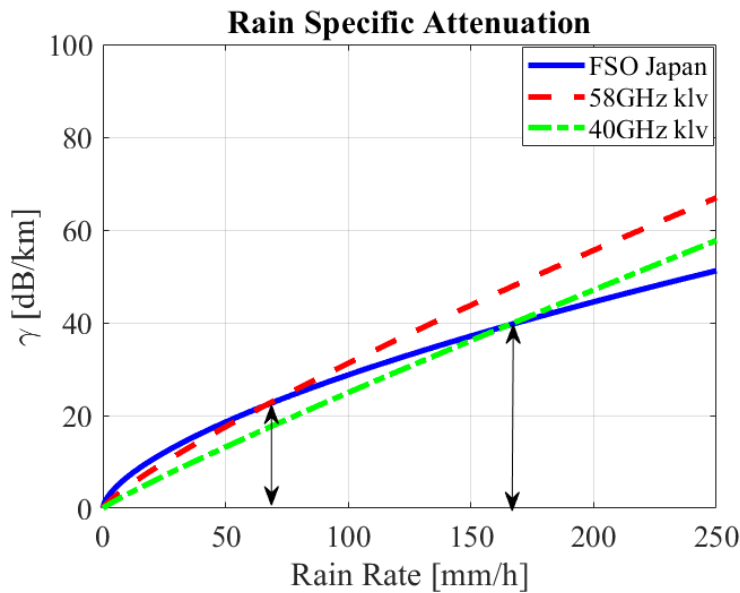


Figure 8. Specific Rain Attenuations for FSO, 40GHz, and 58GHz in KL

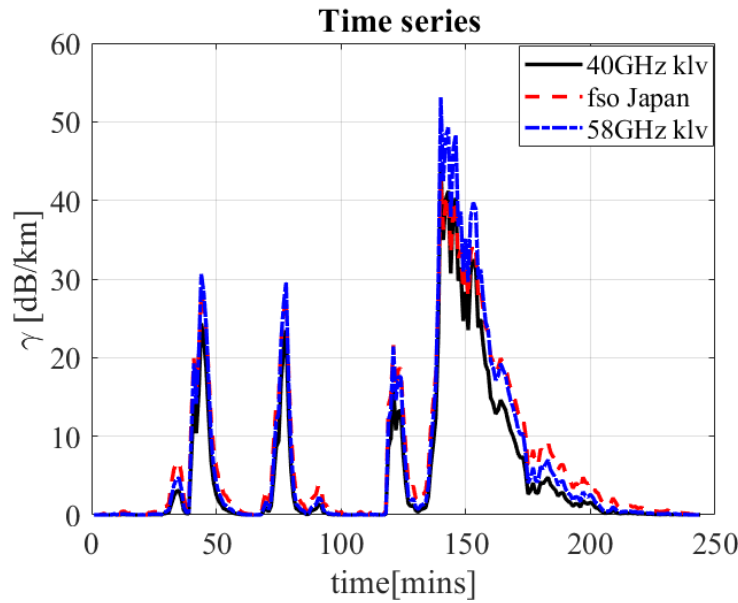


Figure 9. Time Series of Rain Attenuations for FSO, 40GHz, and 58GHz in KL

The CCDFs of the specific rain attenuations for the FSO link, 58 GHz link, and Hybrid system are investigated, as shown in Figure 10. When the time percentage (%) is between 1% and 0.1%, the FSO link provides a slightly higher rain attenuation than the 58 GHz link. Meanwhile, it predicts lower rain attenuations than the RF link at 0.1% and below the time. The values of  $R_{sa}$  for the FSO link and 58 GHz are approximately equal to 35 dB and 42 dB, respectively. Thus, the gain of attenuation due to rain equals about 7 dB. The FSO link can be supplemented with 58 GHz as a radio frequency in a hybrid system to reduce rain attenuation and increase link availability, data transmission rate, and system capacity. Therefore, the link performance improves during high rain rates. Figure 11 displays the relation between the  $P_r$  and rain rate when the transmitter power is up to 100 mw and the link length of 1 Km for FSO and RF 58GHz links. As can be seen here, high rain intensities are produced by low received power. The received powers for FSO link are higher than RF for transmitting power up to 100mw. At rain rate of 100 mm/h and transmitter power of 5, 10, 50, and 100 mw, the received powers for the FSO link are equal to -39dBm, -36 dBm, -29dBm and -26dBm, respectively. Meanwhile, RF links are equal to -70dBm, -67dBm, -60dBm, and -57dBm.

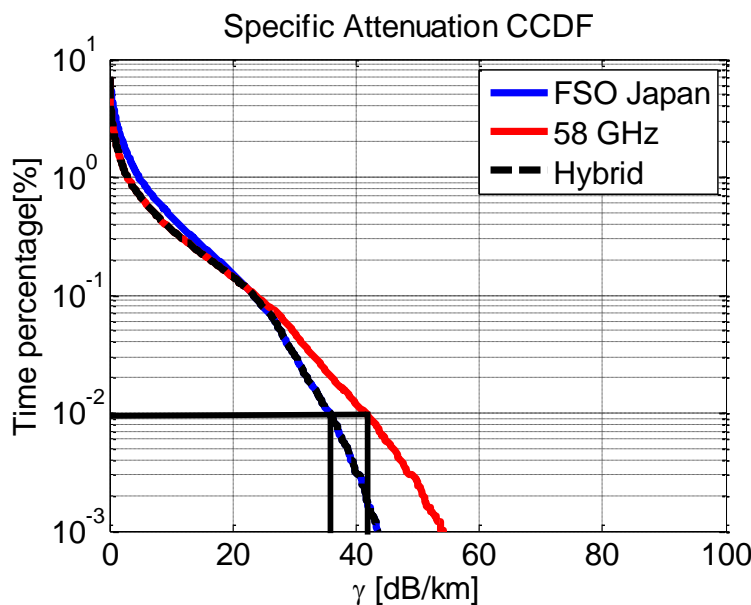


Figure 10. Specific Rain Attenuations for FSO link, 58 GHz link, and Hybrid System in CCDFs.

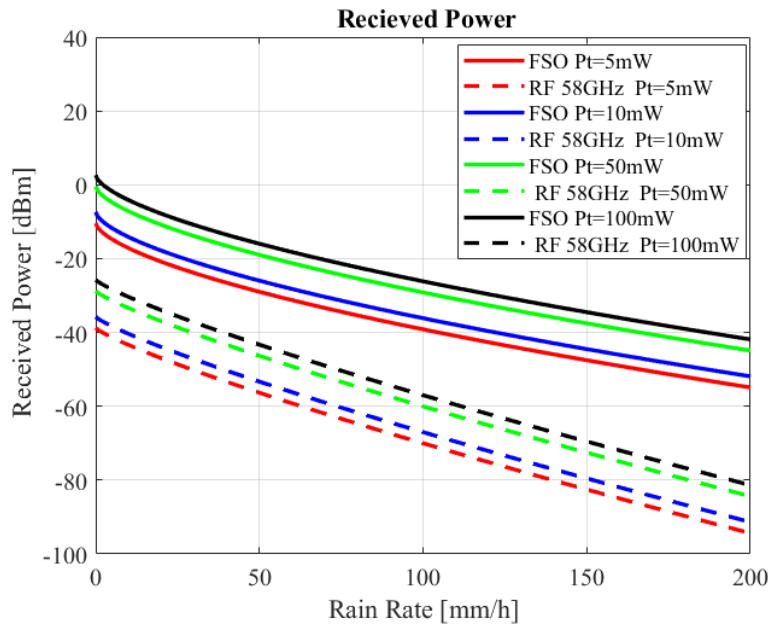


Figure 11. Received Power for FSO link and RF 58 GHz link with Transmitter Powers up to 100 mw and Link Length of 1 Km.

$P_r$  and rain attenuation curve is simulated up to 100mw of  $P_t$ , are shown in Figure 12. High rain attenuations provide low  $P_r$  for both links of FSO and RF at transmitter powers up to 100 mw. The  $P_r$  for the FSO link is higher as compared to the RF link for transmitting power up to 100 mw. For transmitting powers of 5 mw, 10mw, 50 mw, and 100mw at 30 dB of rain attenuation, the  $P_r$  for FSO are equal to -40dBm, -37dBm, -30dBm and -27dBm respectively, and for RF link are equal to -68.8dBm, -65.8dBm, -58dBm and -55.8dBm. The atmospheric attenuation loss will decrease the  $P_r$  at the FSO and RF system receivers. This limits other crucial variables, particularly link margin, which deteriorates the communication link's performance. Reducing link length or increasing transmitted power to compensate for channel attenuation loss will improve  $P_r$ , as raising transmitter power will also increase  $P_r$  at the receiver side.

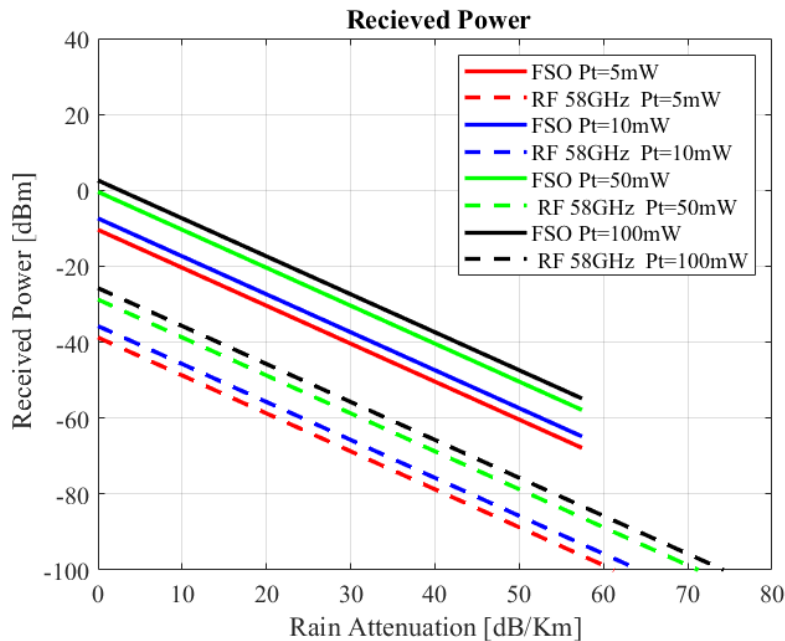


Figure 12. Received Powers versus the Rain Attenuations

There are very slight effects of rain intensities and channel attenuations on SNR. Simulation results in Figure 13&14 show that as rain rate and attenuation increase, SNR decreases slightly. At a 100 mm/h rain rate and transmitter power of 5, 10, 50, and 100 mw, SNR

for the FSO link are equal to -1.9dB, 4dB, 18dB, and 24dB, respectively. At the same time, RF links are equal to 8dB, 11dB, 18dB, and 21dB, respectively. At low transmitted power and heavy rain rates, the SNR for the RF link is higher than that of the FSO link. Meanwhile, SNR for the FSO link is higher than RF for high transmitting power. This is because the total noise power for the FSO receiver is higher than that of the RF receiver. The solution for this issue is to increase transmitter power ( $P_t \geq 100$  mw) or reduce the link distance.

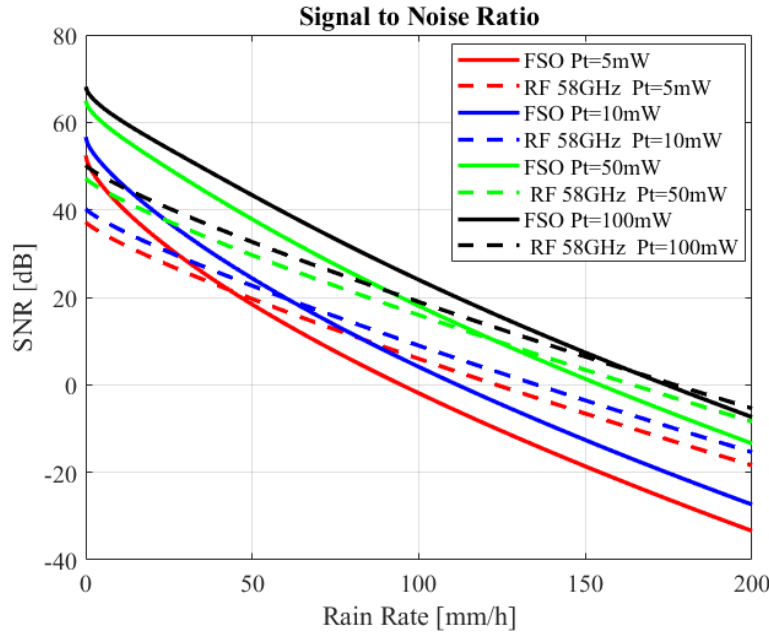


Figure 13. SNR versus the Rain Rate

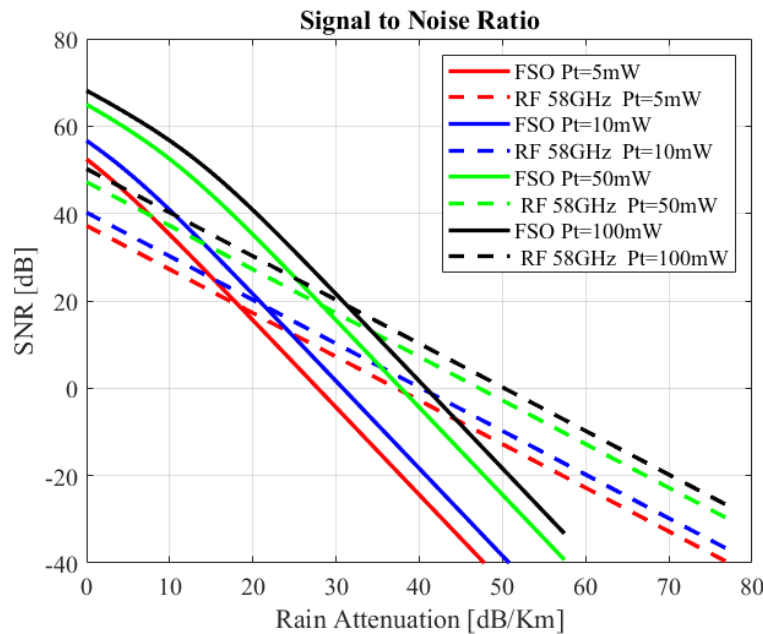


Figure 14. SNR versus the Rain Attenuation

Signals are sent in the space for FSO and RF systems, and channel attenuations may result in losses of transmitted signal. BER is the term used to describe the information loss that occurs in optical and radio transmissions. BER is another crucial communication element that determines the link's dependability and quality. Since BER is inversely correlated with SNR, more attenuation will result in higher BER. Increased noise strength in the signals from the surrounding environment will result in a high BER and decreased system data dependability. The received signal quality will be poor if the BER is high. Figures 15 and 16 demonstrate how BER for

FSO and RF lines increases in tandem with rain rate and attenuation. The BER values for the FSO connection are  $0.34$ ,  $0.21$ ,  $3.3 \times 10^{-5}$ , and  $1.14 \times 10^{-15}$  at a rain rate of  $100 \text{ mm/h}$  and transmitted powers. In the interim, the RF values are  $0.1$ ,  $0.03$ ,  $3.98 \times 10^{-5}$ , and  $1.2 \times 10^{-8}$ , in that order. Increasing transmitter power can also result in an improvement in the BER. SNR and BER have an antagonistic connection. SNR declines as the BER rate rises.

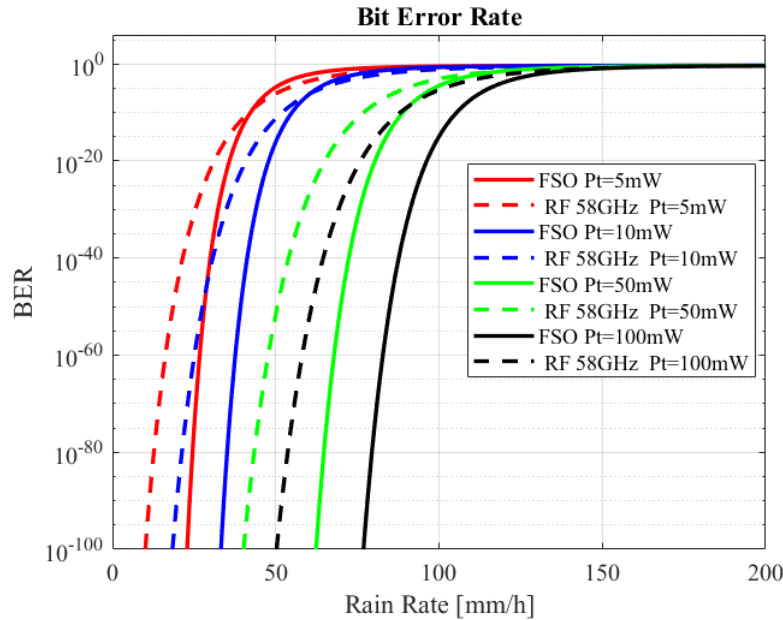


Figure 15. Bit Error Rate versus the Rain Rate

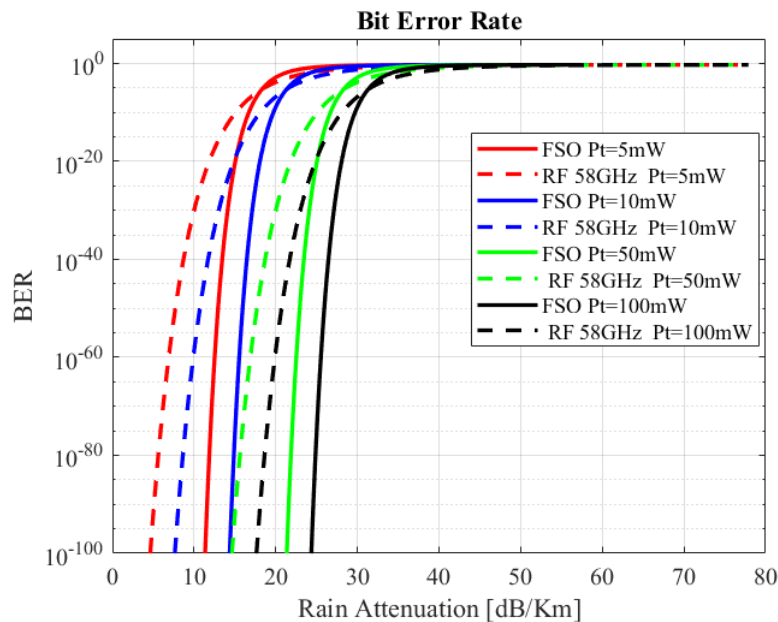


Figure 16. Bit Error Rate versus the Rain Attenuation

The comparison of the proposed model and related work of Hybrid FSO/58GHz and Hybrid FSO/10GHz, respectively, is shown in Figure 17. The simulation model of related work was done in Alexandria, Egypt [23]. The authors evaluated the system by promoting a hybrid model under rainy weather conditions. Both models have used an NRZOOK modulation technique, transmitter power of  $5 \text{ mw}$ , and path length of  $1 \text{ Km}$ . As seen here, BER for FSO links of both models are almost equal at high rain intensities ( $R > 100 \text{ mm/h}$ ); meanwhile, it is higher for RF 58GHz compared to  $10 \text{ GHz}$ . This is because an RF link at  $58 \text{ GHz}$  predicts higher attenuation than  $10 \text{ GHz}$  under heavy rain conditions. Hybrid FSO/58GHz provides lower BER as compared to Hybrid FSO/10GHz at low rain intensities ( $R < 60 \text{ mm/h}$ ). At a rain rate of  $43 \text{ mm/h}$  ( $R=43 \text{ mm/h}$ ), the BER of Hybrid FSO/58GHz for the FSO link is equal to RF 58GHz to  $5.6 \times 10^{-10}$ ; meanwhile, for FSO and RF  $10 \text{ GHz}$  of related Hybrid are equal to  $0.21$  and  $4.7 \times 10^{-4}$  respectively.

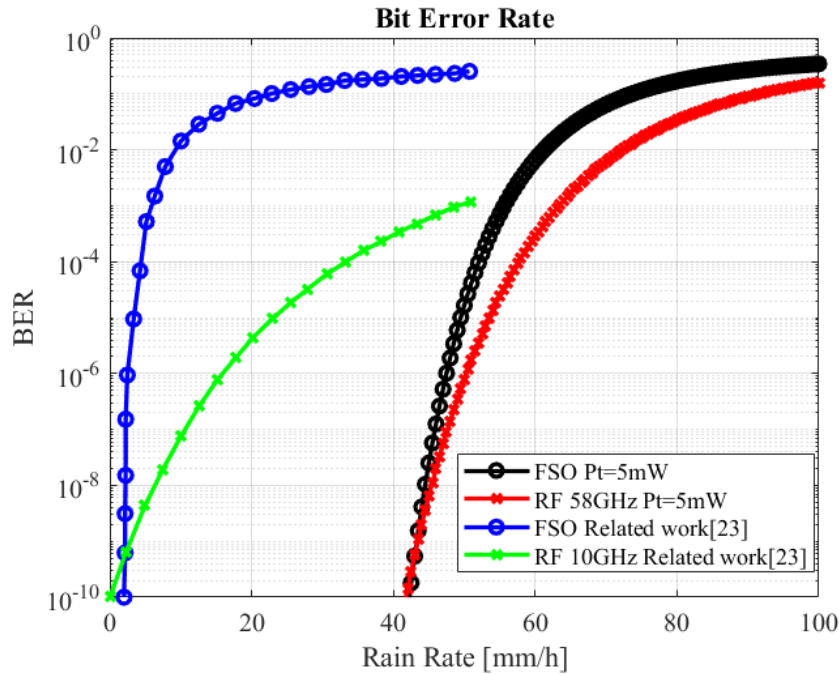


Figure 17. The Comparison between Proposed Hybrid FSO/58GHz and Hybrid FSO/10GHz related work for Transmitting Power of 5 mW and Link Length of 1 Km.

System availability that meets commercial carrier requirements may be ensured through the use of RF and FSO connectivity. Nevertheless, the available RF connection's bandwidth is not fully utilised while the primary FSO is in use. For hybrid systems, a switching approach has been devised to optimise the utilisation of this bandwidth. When the FSO system usually operates, more data is transmitted across the RF connection to maximise the system's capacity. As seen in Figure 18, the signal level at the receiver ( $P_r$ ) is monitored using a certain threshold setting. The model switches to the RF if the received signal intensity on the FSO link drops below this threshold ( $P_{thFSO}$ ). Following this changeover, test data is sent over the FSO, and data is sent over the RF. Until the signal recovers and load sharing between two separate data streams is reinstated, the FSO's received signal is continually observed and compared to a higher threshold value. As a result, the system may continue to function even if severe rain causes an interruption to the FSO. The same technique is used to stop repetitive switching when an RF fails, comparing the received signal strength by the RF to a higher threshold.

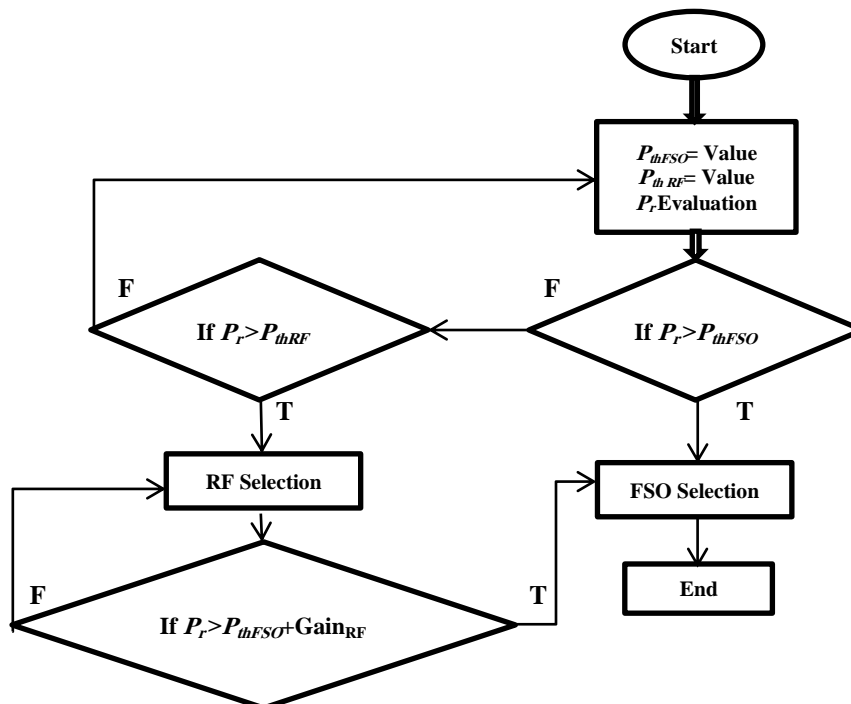


Figure 18. Algorithm switching For Hybrid FSO/RF system.

## VI. CONCLUSION

The study of rain attenuation for RF links in Kuala Lumpur, particularly at frequencies from 10 to 50 GHz and at 58 GHz, reveals that attenuation is negligible below 10 GHz but significant at higher frequencies. The 58 GHz frequency has been identified as suitable for enhancement with an FSO link in a hybrid FSO/58 GHz system. This hybrid system consistently provides the lowest rain attenuation compared to individual FSO and 58 GHz links, regardless of rain intensity. A notable 7 dB increase in rain attenuation between the FSO link and 58 GHz was observed. Performance metrics such as received power, SNR, and BER were analysed, demonstrating improved system performance under heavy rain conditions. Compared to related models, the current hybrid FSO/58 GHz system achieves a lower bit error rate during light to moderate rain ( $R < 60$  mm/h) than the hybrid FSO/10 GHz system.

## REFERENCES

- [1] S. A. H. Mohsan, M. A. Khan, and H. Amjad, "Hybrid FSO/RF networks: a Review of Practical constraints, Applications and Challenges," *Optical Switching and Networking*, vol. 47, p. 100697, Feb. 2023.
- [2] G. Gautam, N. Sharma, and S. Kumar, "Radio over FSO System for 5G Wireless Communication," 2022 13th International Conference on Computing Communication and Networking Technologies (ICCCNT), pp. 1–6, Oct. 2022.
- [3] T. Sharma, A. Chehri, and P. Fortier, "Review of Optical and Wireless Backhaul Networks and Emerging Trends of next Generation 5G And 6G Technologies," *Transactions on Emerging Telecommunications Technologies*, vol. 32, no. 3, p. e415, Oct. 2020.
- [4] A. Z. Suriza, I. Md Rafiqul, A. K. Wajdi, and A. W. Naji, "Proposed Parameters of Specific Rain Attenuation Prediction for Free Space Optics Link Operating in Tropical Region," *Journal of Atmospheric and Solar-Terrestrial Physics*, vol. 94, pp. 93–99, Mar. 2013.
- [5] Mohammed, et al., "Generation of a New Hybrid Subcarrier multiplexing–SAC-OCDMA System Based on FSO," *Journal of Theoretical and Applied Information Technology*, vol. 58, no. 2, pp. 389–396, 2013.
- [6] S. A. Zabidi, Md. R. Islam, W. Al-Khateeb, and A. W. Naji, "Analysis of Rain Effects on Terrestrial Free Space Optics Based on Data Measured in Tropical Climate," *IJUM Engineering Journal*, vol. 12, no. 5, Jan. 2012.
- [7] Willebrand, Heinz, and B. S. Ghuman, *Free Space Optics: Enabling Optical Connectivity in today's Networks*. SAMS Publishing, 2002.
- [8] M. Rafiqul, "Rain Attenuation Prediction for Terrestrial Microwave Links Based on Rain Rate and Rain Attenuation Measurements in a Tropical Region," University of Technology Malaysia, Johor Bahru, 2000.
- [9] A. M. Rwaidi, A. M. Matarneh, and S. S. Alja'afreh, "The Performance of Millimeter-Wave over FSO Communication Systems under Adverse Atmospheric Conditions for 6G Applications," 2023 14th International Conference on Information and Communication Systems (ICICS). IEEE, pp. 1–6, Nov. 2023.
- [10] S. Kaur and J. Kaur, "Rain Attenuation Analysis of a Radio over Free Space Optics System considering Diverse Regions," *Journal of Optical Technology*, vol. 90, no. 8, pp. 476–476, Aug. 2023.
- [11] Recommendation, I, "Prediction Methods Required for the Design of Terrestrial free-space Optical Links," *International Telecommunication Union*, vol. 1814, 2007.
- [12] R. K. Crane, "Rain Attenuation models: Attenuation by Clouds and Rain," *Propagation Handbook for Wireless Communication System* 225, vol. 225, no. 280, 2003.
- [13] José Manuel Riera et al., "Characterization of Rain Attenuation in 80–200 GHz from Experimental Drop Size Distributions," *IEEE Transactions on Antennas and Propagation*, vol. 71, no. 5, pp. 4371–4379, May 2023.
- [14] E. Alozie et al., "A Review on Rain Signal Attenuation Modeling, Analysis and Validation Techniques: Advances, Challenges and Future Direction," *Sustainability*, vol. 14, no. 18, p. 11744, Sep. 2022.
- [15] M. A. Samad, F. D. Diba, and D.-Y. Choi, "A Survey of Rain Attenuation Prediction Models for Terrestrial Links—Current Research Challenges and State-of-the-Art," *Sensors*, vol. 21, no. 4, p. 1207, Feb. 2021.
- [16] O. Zahid and S. Salous, "Long- Term Rain Attenuation Measurement for Short- Range mmWave Fixed Link Using DSD and ITU- R Prediction Models," *Radio Science*, vol. 57, no. 4, Apr. 2022.
- [17] Marzuki, T. Kozu, T. Shimomai, H. Hashiguchi, W. L. Randeu, and M. Vonnisa, "Raindrop Size Distributions of Convective Rain over Equatorial Indonesia during the First CPEA Campaign," *Atmospheric Research*, vol. 96, no. 4, pp. 645–655, Jun. 2010.
- [18] R. P. Series, "Propagation Data and Prediction Methods Required for the Design of Terrestrial line-of-sight Systems," *Recommendation ITU-R*, vol. 530–12, 2015.
- [19] V. Kvicera, M. Grabner, and O. Fiser, "Long-Term Propagation Statistics and Availability Performance Assessment for Simulated Terrestrial Hybrid FSO/RF System," *EURASIP Journal on Wireless Communications and Networking*, vol. 2011, no. 1, pp. 1–9, Mar. 2011.
- [20] F. Nadeem, V. Kvicera, M. Awan, E. Leitgeb, S. Muhammad, and G. Kandung, "Weather Effects on Hybrid FSO/RF Communication Link," *IEEE Journal on Selected Areas in Communications*, vol. 27, no. 9, pp. 1687–1697, Dec. 2009.
- [21] T. H. Carbonneau and D. Wisely, "Opportunities and Challenges for Optical wireless: the Competitive Advantage of Free Space Telecommunications Links in today's Crowded Marketplace," *Wireless Technologies and systems: millimeter-wave and Optical* 3232, pp. 119–128, Jan. 1998.
- [22] W. M. R. Shakir, "Performance Analysis of the Hybrid MMW RF/FSO Transmission System," *Wireless Personal Communications*, vol. 109, no. 4, pp. 2199–2211, Aug. 2019.
- [23] Sherif Ghoname, H. A. Fayed, A. Abd, and M. H. Aly, "Performance Evaluation of an Adaptive Hybrid FSO/RF Communication System: Impact of Weather Attenuation," *Electrical & Computer engineering/Iranian Journal of Science and technology. Transactions of Electrical Engineering*, vol. 44, no. 1, pp. 119–128, Aug. 2019.

- [24] A. A. Basahel, Islam Md. Rafiqul, Mohamed Hadi Habaebi, and S. A. Zabidi, "Availability Modelling of Terrestrial Hybrid FSO/RF Based on Weather Statistics from Tropical Region," *IET Communications*, vol. 14, no. 12, pp. 1937–1941, Jul. 2020.
- [25] H. Kashif, M. N. Khan, and A. Altalbe, "Hybrid Optical-Radio Transmission System Link Quality: Link Budget Analysis," *IEEE Access*, vol. 8, pp. 65983–65992, 2020.
- [26] S. Magidi and A. Jabeena, "Analysis of Hybrid FSO/RF Communication System under the Effects of Combined Atmospheric Fading and Pointing Errors," *Optical and Quantum Electronics*, vol. 54, no. 4, Mar. 2022.
- [27] S. M. Yasir, N. Abas, A. Rahman, and M. S. Saleem, "Simulation Analysis of Adaptive FSO/RF Hybrid Link under Diverse Weather Conditions of Lahore, Pakistan," *Results in Optics*, vol. 2, p. 100047, Jan. 2021.
- [28] D. Verma and S. Prince, "Performance Analysis of a Hybrid FSO/mmWave/THz System for Short-Range Communication under Rain and Fog Conditions," *Physica Scripta*, vol. 98, no. 11, pp. 115506–115506, Oct. 2023.
- [29] Shakshi Ghatwal and H. Saini, "A Hybrid FSO/RF Communication System with DSP for Long Haul Communication," *Journal of Optical Communications*, Dec. 2023.
- [30] S.-W. Ho and G. Bolding, "On the Statistical Property of Hybrid E-Band/Free Space Optical Systems," *IEEE Transactions on Wireless Communications*, pp. 1–1, Jan. 2024.
- [31] M. Ali Amirabadi and V. Tabataba Vakili, "Performance Analysis of a Novel Hybrid FSO/RF Communication System," *IET Optoelectronics*, vol. 14, no. 2, pp. 66–74, Apr. 2020.
- [32] P. H. Mohamed, M. A. El-Shimy, Hossam M.H. Shalaby, and Hassan Nadir Kheirallah, "Hybrid FSO/RF System over Proposed Random Dust Attenuation Model Based on real-time Data Combined with G–G Atmospheric Turbulence," *Optics Communications*, vol. 549, pp. 129891–129891, Dec. 2023.
- [33] N. M., H. Sizon, and F. Fornel, "Propagation of Optical and Infrared Waves in the Atmosphere," *Proceedings of the Union Radio Scientifique Internationale*, 2005.
- [34] R. I. T. U. R., "Specific Attenuation Model for Rain for Use in Prediction Methods," *Recommendation ITU-R*, vol. 838–3, 2005.
- [35] B. Olivier, et al, *Free-space optics: Propagation and Communication*, vol. 91. John Wiley & Sons, 2010.
- [36] Bohren, Craig F, and Donald R. Huffman, *Absorption and Scattering of Light by Small Particles*. John Wiley & Sons, 2008.
- [37] T. W. Harrold, "Attenuation of 8.6 mm-wavelength Radiation in Rain," *Proceedings of the Institution of Electrical Engineers*, vol. 114, no. 2, p. 201, 1967.
- [38] Lakshmi S. K., Yee H. L., and J. Ong, "Truncated Gamma Drop Size Distribution Models for Rain Attenuation in Singapore," *IEEE Transactions on Antennas and Propagation*, vol. 58, no. 4, pp. 1325–1335, Apr. 2010.
- [39] H. Ab, A. M. Nor, and Suriza Ahmad Zabidi, "Performance Analysis of Free Space Optics Link under the Effect of Rain Attenuation," *The International Islamic University Malaysia Repository (The International Islamic University Malaysia)*, pp. 391–396, Jun. 2021.
- [40] R. Al-Dabbagh and H. Al-Raweshidy, "Millimeter-Wave Transmission Technologies over Fiber/FSO for 5G+ Networks," 2021 IEEE 11th International Conference on Consumer Electronics (ICCE-Berlin), Nov. 2021.
- [41] E. B. Bakırcı, E. S. Ahrazoğlu, İ. Altunbaş, and E. Erdoğan, "Outage Probability Analysis of Triple-Hybrid RF/FSO/THz Communication System," 2024 32nd Signal Processing and Communications Applications Conference (SIU). IEEE, pp. 1–4, May 2024.
- [42] O. Aboelala, I. E. Lee, and G. C. Chung, "A Survey of Hybrid Free Space Optics (FSO) Communication Networks to Achieve 5G Connectivity for Backhauling," *Entropy*, vol. 24, no. 11, p. 1573, Oct. 2022.
- [43] G. Hu, C. Chen, and Z. Chen, "Free-Space Optical Communication Using Visible Light," *Journal of Zhejiang University-SCIENCE a*, vol. 8, no. 2, pp. 186–191, Feb. 2007.
- [44] W. R. Leeb, "Comparison of Microwave and Light Wave Communication Systems in Space Applications," *Optical Engineering*, vol. 46, no. 1, pp. 015003–015003, Jan. 2007.
- [45] Osayd Kharraz and David Ian Forsyth, "PIN and APD Photodetector Efficiencies in the Longer Wavelength Range 1300–1550 Nm," *Optik*, vol. 124, no. 16, pp. 2574–2576, Aug. 2013.
- [46] K. Ajaybeer and M. L. Singh, "Performance Evaluation of Free Space Optics (FSO) and Radio Frequency Communication System Due to Combined Effect of Fog and Snow," *International Conference on Recent Advances and Future Trends in Information Technology*, 2012.
- [47] H. Y. Lam, L. Luini, J. Din, C. Capsoni, and A. D. Panagopoulos, "Preliminary Investigation of Rain Cells in Equatorial Malaysia for Propagation Applications," 2013 IEEE International RF and Microwave Conference (RFM). IEEE, pp. 243–246, Dec. 2013.
- [48] H. Y. Lam, L. Luini, J. Din, C. Capsoni, and A. D. Panagopoulos, "Investigation of Rain Attenuation in Equatorial Kuala Lumpur," *IEEE Antennas and Wireless Propagation Letters*, vol. 11, pp. 1002–1005, 2012.
- [49] D. Jafri, "Influence of Rainfall Drop Size Distribution on Attenuation at Microwave Frequencies in a Tropical Region," *Doctoral Dissertation*, UTM, 1997.
- [50] A. K. Rahman, A. Kwang, R. Endut, S. A. Aljunid, N. Ali, and M. Rashidi, "Prediction Rain Attenuation Effect on Free Space Optical Communication Kuching/Samarahan Region," *AIP Conference Proceedings*, vol. 2898, no. 1, Jan. 2024.
- [51] S. Attri, C. Madhu, and D. Kaur, "Performance Analysis of 4QAM-OFDM-FSO Link under Rain Weather Conditions," *Journal of Optical Communications*, vol. 0, Apr. 2024.